Experimental Investigation of the Possibility of Transporting a Droplet Over a Hydrophilic Spot in Digital Microfluidics

E. Samiei* and M. Hoorfar**

*, **University of British Columbia, 3333 University Way, Kelowna, BC, Canada
*ehsan.samiei@ubc.ca
**mina.hoorfar@ubc.ca

ABSTRACT

This paper studies the transport of a water droplet over a hydrophilic spot, representing the sensing surface of a biosensor. This is important since label-free biosensors, which mostly have a hydrophilic sensing surface (hindering droplet manipulation on the chip), are suitable for digital microfluidic (DMF) devices proposed for real time biosensing for point of care applications. A closed system with an array of electrodes has been designed and the hydrophilic spot created on the top plate was placed above one of the middle actuating electrodes. The bottom plate is fabricated by standard photolithography from a copper coated glass slide, coated with a dielectric and a Teflon layer. The top plate is a Teflon coated ITO glass slide. The hydrophilic spots are created on the top plate by removing the Teflon layer using a micro-machining laser. The effects of the droplet and electrode sizes, the gap between the two plates and the geometry of the hydrophilic spots on droplet manipulation are investigated.

Keywords: digital microfluidics, hydrophilic spot, label-free biosensors, geometrical parameters

1 INTRODUCTION

In recent years miniaturization has become a trend in design and fabrication of devices used in most fields of science and technology. As a result, Lab on a chip (LOC) devices were introduced to replace old fashioned macro-scale biochemical fluidic operations with rapid and accurate on-chip processes requiring less power and a smaller sample size.

The original LOC devices performed biochemical processes (e.g., mixing, separation, purification, etc.) through manipulation of microflow in pre-etched microchannels using micro-valves and micro-pumps. These groups of LOC devices are referred to as continuous microfluidics. Despite the general success of such devices, the permanently etched channels limit flexibility and reconfigurability of continuous microfluidic devices. Also, fabrication of micro-valves and micro-pumps in such a small scale has its own complexity [1]. Free from these limitations and complexities, digital microfluidics (DMF) has attracted attentions in the past decade. DMF devices perform fluidic operations on the chip simultaneously without cross contamination. These devices work based on manipulation of discrete droplets over an array of patterned electrodes. This makes DMF devices flexible as a single chip can be used for different applications [1, 2]. Also, power and sample consumptions in DMF devices are reduced by several orders of magnitude [2].

Digital microfluidics has been used in a variety of biochemical applications including cell-based analysis [3, 4], enzymatic and chemical reactions [5, 6], DNA applications [7], etc. In most applications fluorescence microscopy is used for detection [3, 4, 7] of molecules of interest. This sensing mechanism needs the use of fluorescent dyes which might affect the chemical and electrical behavior of the sample. Thus, highly sensitive label-free sensors, which are based on electrical [8], mechanical [9] or optical [10] principles, have been introduced to replace fluorescent-based sensors in DMF platforms. Also, label-free sensors can readily be implemented into DMF platforms as the sensing surface of these sensors can be placed on the top plate having no patterned electrodes. A common feature of most label-free biosensors is that they have a sensing surface which is in direct contact with the sample liquid. However, the sensing surface is fabricated mainly by hydrophilic metals and semiconductors [8-10] which can compromise droplet motion on DMF chips. Therefore, prior to integration of these kinds of sensors into DMF devices, the possibility of droplet manipulation with the presence of a hydrophilic zone on the chip surface should be studied.

In this work, droplet actuation over a hydrophilic spot placed on the top plate of a DMF chip, representing the sensing surface of the label-free biosensors, is studied experimentally. The effects of geometrical parameters (electrode and droplet sizes, the gap between the two plates, and the position the spot) are also studies. For each configuration a threshold hydrophilic surface area, below which the droplet can be transported, will be identified.

2 THEORY

The most common method for droplet actuation in DMF devices is electrowetting on dielectric (EWOD) [11]. A closed configuration, in which the droplet is sandwiched between top and bottom plates, is used in this study. The actuating electrodes are patterned on the bottom plate, covered with a dielectric layer. The top plate is covered with ITO used as the ground electrode. Both plates are coated with a layer of Teflon to make their surfaces hydrophobic (facilitating the droplet motion). If a droplet of a conductive liquid is placed between the two plates (surrounded by air) there will be interfacial energy between each pair of the phases which are related to the contact angle through Young's equation [12].

$$\cos\theta_0 = \frac{\gamma_{sg} - \gamma_{sl}}{\gamma_{\lg}} \tag{1}$$

where θ_0 is the equilibrium contact angle. γ_{lv}, γ_{sl} and γ_{sg} are the liquid-vapor, solid-liquid, and solid-vapor interfacial tensions, respectively. By applying a potential between the droplet and the electrode, electric charges will be accumulated on the electrode surface and the liquid-dielectric interface, forming a capacitor. The electrostatic energy of the capacitor at the liquid-solid interface decreases the apparent solid-liquid interfacial energy, and as the side effect there will be a change in the apparent contact angle. Following equation represents the change in the solid-liquid interfacial energy [12]:

$$\Delta\gamma_{sl} = \frac{\varepsilon_0\varepsilon_d}{2d}U^2 \tag{2}$$

where $\Delta\gamma_{sl}$ represents the change in the solid-liquid interfacial tension, U is the applied potential, ε_0 is the permittivity of the vacuum, ε_d and d are the dielectric constant and the thickness of the dielectric layer, respectively.

3 FABRICATION AND EXPERIMENTAL SET UP

The bottom plate used is a copper coated glass slide on which the electrodes are patterned by standard photolithography. A layer of photoresist S1805 (MicroChem Corp.) used as the dielectric layer is spun (3000 *rpm* for 60 *s*) and baked (30 *min* at 95°*C*) on the patterned electrodes. The bottom plate is then coated (spun at 2500 *rpm* for 60 *s*) with a solution of Teflon AF 1600 (DuPont) of a concentration of 3 *wt%* which was baked for 2 *hrs* at 95°*C*. An ITO coated glass slide (S_iO_2 passivated, Rs = 4–8Ω) covered by a Teflon layer (same as the bottom plate) is used as the top plate. A micro-machining laser (Oxford Lasers Ltd.) is used to remove the Teflon layer from the desired areas to pattern the hydrophilic spots on the top plates. The electrodes are then connected to an electrical potential supplier and a signal function generator (Tektronix AFG3021B0), connected to an amplifier (TREK PZD700). The experiments are monitored by an Apo-zoom microscope (Leica Z6 APO) equipped with a high speed camera.

4 EXPERIMENTS

In order to study the transport of a droplet over a hydrophilic spot, an array of 5 square electrodes is designed (Fig. 1). Two designs with the electrode sizes of L_E =1 mm and 2 mm are considered. The hydrophilic spot (which is patterned on the top plate) is placed on the top of the middle electrode (shown by a circle in Fig. 1). In this study 19 rectangular hydrophilic zones with the length/width aspect ratio of 2 are patterned (Fig. 2). The lengths of these rectangles are between L_H=1.1 *mm* (the largest rectangle) to 0.2 *mm* (the smallest rectangle) with an increment of 0.05 *mm* between two consecutive designs. The spots are located on the top of the desired electrode in a way that the length of the spot is parallel to the flow direction.

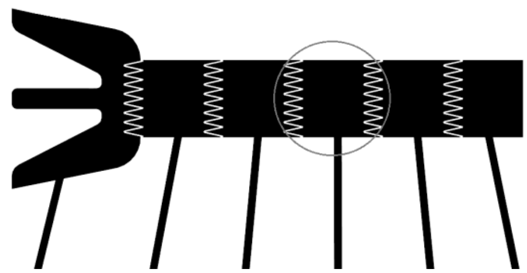

Figure 1: The designed array of electrodes. The circle shows the electrode above which the hydrophilic spot is placed.

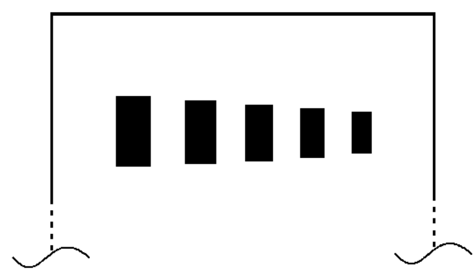

Figure 2: A schematic of the patterned hydrophilic spots on the top plate.

For each electrode size two droplet sizes are considered: for the 1mm electrode design, the droplet volumes are V_d =300 and 500 *nL*; whereas, the droplet sizes of V_d=1 and 1.5 μL were considered for the 2 *mm* electrode design. For each set of the electrodes, droplet and hydrophilic spot sizes the experiments were conducted for different gap sizes (*t*) between the two plates. Three locations are chosen for the position of the spot: middle of the electrode, close to the leading edge of the electrode (defined based on direction of the droplet motion), and close to the rear edge of the electrode. These locations are denoted by *M*, *L*, and *R*, respectively. An AC puls signal with the amplitude of 200 *V* p-p and the frequency of *f*=1 *kHz* was used to actuate the electrodes. Each experiment was repeated at least three times to assure the reproducibility of the results.

5 RESULTS AND DISCUSSION

The first set of experiments was conducted for the droplet size of 300 *nL* on the 1mm electrode design and 19 hydrophobic spots, located on the top plate. It was observed that for the smallest hydrophilic spot size (0.2×0.1 *mm*), the droplet moved over the spot successfully. For this set of parameters the largest spot for which the droplet could be transported was found to be 0.65×0.325 *mm*. For each hydrophilic spot size the experiment was conducted for different gap sizes between the two plates. Fig. 3 shows the minimum gap size versus the spot size for which droplet transport was successfully achieved. The larger the gap size the easier the droplet transport. In essence, for each spot size, there is a minimum gap size below which the droplet cannot be transported over the hydrophilic zone. For larger hydrophilic spots the minimum gap is larger. It is evident that the minimum gap size increases with increasing the spot size. For this small droplet, necking and hence droplet splitting does not occur due to the dominant effect of surface tension. For the spots larger than 0.65×0.325 *mm*, the droplet cannot be transported over the hydrophilic zone even for larger gap sizes.

To study the effects of the droplet size, the experiments were repeated on the 1 *mm* electrode design for the droplet size of 500 *nL*. The minimum gap size as a function of spot size is shown in Fig. 3. The comparison between the results obtained for the two droplet sizes shows that for the larger droplet the minimum gap is larger. As the gap size decreases the larger droplet becomes unstable upon actuation of the adjacent electrode. This results in droplet splitting over the hydrophilic spot. However, for this case the droplet can be handled over larger hydrophilic spots. This means transport of the larger droplet is feasible, if the gap size is chosen large enough to prevent splitting. This could be because of the higher electrowetting force acting on the larger droplet due to a larger contact area with the adjacent actuated electrode. The largest spot over which the droplet can be transported is found to be 1.0×0.5 *mm* for any gap sizes tested here.

To study the effects of the electrode size, the above experiments were repeated on the 2 *mm* electrode design. Two sizes of droplet (1 μL and 1.5 μL) were considered. Fig. 3 includes the results of the minimum gap size versus the hydrophilic spot size obtained for the 1 μL droplet. For this size, the larger the spot size the larger the gap for which droplet transport can be achieved. The comparison between the results obtained for 1 μL droplet on the 2 *mm* electrode with those obtained for the 500 *nL* droplet on the 1 *mm* electrode (which have the same V_d/L_E ratio) shows that the minimum gap sizes, for which the transport is successfully achieved, are smaller for 2 *mm* electrode size (even with larger V_d). This could be due to the fact that upon actuation of the adjacent electrode the droplet elongates (because of the effect of EWOD), and for the larger electrode size, the width of the elongated droplet is larger, preventing necking and splitting over the hydrophilic spot. Thus, by increasing the electrode and droplet sizes, transport of the droplet over a hydrophilic spot will be easier and the threshold spot size will increase (while the minimum gap for the same spot size is smaller). For this case, the threshold spot size is larger than the maximum spot size (i.e. 1.1 ×0.55 *mm*).

Finally, a droplet of 1.5 μL size is tested on the 2 *mm* electrode design (see Fig. 3). For this case, the droplet was easily moved over all the patterned hydrophilic spots, and the threshold spot size was also found to be larger than 1.1 ×0.55 *mm*. The comparison between the results obtained for the 2 *mm* electrode design for two droplet sizes (1 μL and 1.5 μL) shows that for the same spot size, the minimum gap size is larger for the larger droplet. For the gap sizes smaller than this minimum size, droplet splitting occurs as shown in Fig. 4.

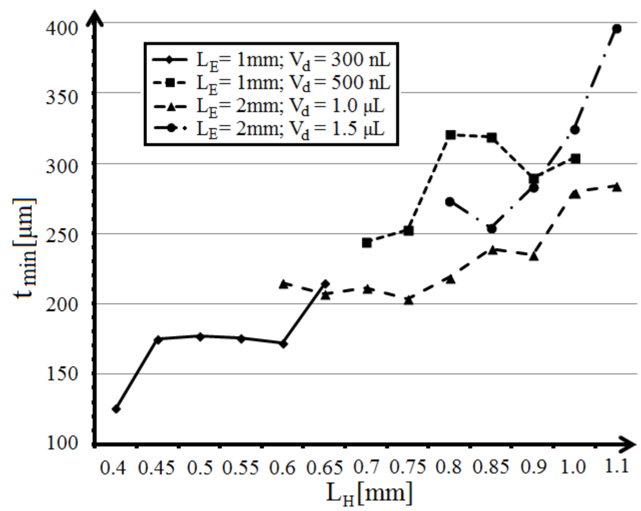

Figure 3: Minimum gap size as a function of maximum hydrophilic spot size for the cases of (a) L_E=1 *mm* and V_d= 300 *nL*, (b) L_E=1 *mm* and V_d= 500 *nL*, (c) L_E=2 *mm* and V_d= 1.0 μL, and (d) L_E=2 *mm* and V_d= 1.5 μL.

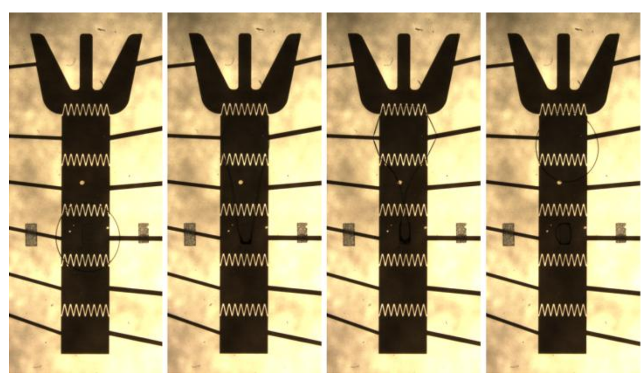

Figure 4: Droplet motion and splitting over a hydrophilic spot (Left to right) occurred for the experimental parameters of L_E=2 *mm*, V_d= 1.5 μL, L_H=0.85 *mm* and t=251.43 μm.

The effect of the position of the hydrophilic spot (denoted by *M*, *L*, and *R*) on droplet transport was also studied for three cases of the electrode, droplet and hydrophilic sizes of (a) L_E=1 *mm*, V_d= 300 *nL* and L_H=0.35 *mm*, b) L_E=2 *mm*, V_d= 1.0 μL and L_H=0.65 *mm*, and c) L_E=2 *mm*, V_d= 1.0 μL and L_H=0.8 *mm*. Fig. 5 shows the minimum gap size for each position for the above three cases. The results show that droplet transport is easier when the hydrophilic spot is located in the middle of the electrode. For the rear position (*R*), the distance of the spot from the actuated electrode is large compared to the middle position. This reduces the effect of EWOD due to the decrease in the contact area with the actuating electrode, requiring larger gap sizes to transport the droplet. For the leading position (*L*), the spot is close to the actuated electrode. Thus, there is not enough distance to remove the droplet from the spot unless the gap size is increased.

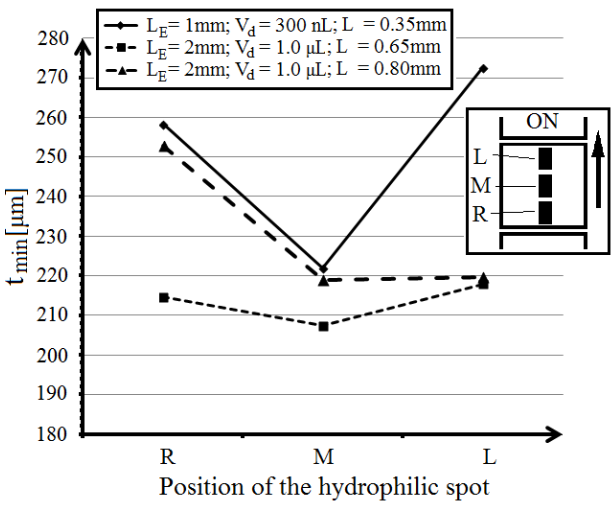

Figure 5: Minimum gap size for each position of hydrophilic spot for three cases of (a) L_E=1 *mm* and V_d= 300 *nL* and L_H=0.35 *mm*, b) L_E=2 *mm*, V_d= 1.0 μL and L_H=0.65 *mm* and c) L_E=2 *mm*, V_d= 1.0 μL and L_H=0.8 *mm*.

6 CONCLUSIONS

Droplet transport over a hydrophilic spot (representing the sensing surface of a label-free biosensor) patterned on the top plate of a DMF chip is studied experimentally. The effects of the parameters such as electrode size, droplet volume, hydrophilic spot size and position, and the gap size between the top and bottom plates are studied. Based on the results the following conclusions can be drawn:

For each set of parameters there is a threshold size for the hydrophilic spot below which the droplet can be transported over the spot without splitting. An increase in the gap size facilitates droplet transport and results in a larger threshold spot size. For the gap sizes below the minimum size, droplet splitting over the hydrophilic spot occurs upon actuating the adjacent electrode. For larger electrode and droplet sizes, the threshold spot size increases. For specific electrode and spot sizes, transport of larger droplets requires larger gap sizes to prevent droplet splitting over the hydrophilic spot. Finally, the study of the effect of the position of the hydrophilic spots shows that droplet transport is easier when the spot is located in the middle of the electrode.

REFERENCES

[1] R. B. Fair, " Digital microfluidics: is a true lab-on-a-chip possible? ", Microfluid Nanofluid, 3, 245-281, 2007.

[2] K. Choi, A. H. C. Ng, R. Fobel and A. R. Wheeler, " Digital Microfluidics", Annu. Rev. Anal. Chem., 5, 413-440, 2012.

[3] G. J. Shah and C. J. Kim, " Meniscus-assisted high-efficiency magnetic collection and separation for ewod droplet microfluidics", J. Microelectromechanical Sys., 18, 2, 363-375, 2009.

[4] S. Park, P. A. L. Wijethunga, H. Moon and B. Han, " On-chip characterization of cryoprotective agent mixtures using an EWOD-based digital microfluidic device", Lab Chip, 11, 2212-2221, 2011.

[5] R. B. Fair et al., "Chemical and biological applications of digital microfluidic devices", IEEE Design & Test, 24, 1, 10-24, 2007.

[6] P. Y. Keng et al., " Micro-chemical synthesis of molecular probes on an electronic microfluidic device", PNAS, 109, 690-695, 2012.

[7] E. Wulff-Burchfield et al., " Microfluidic platform versus conventional real-time polymerase chain reaction for the detection of Mycoplasma pneumoniae in respiratory specimens", Diagnostic Microbiology and Infectious Disease, 67, 22–29, 2010.

[8] K. W. Lee, S. J. Choi, J. H. Ahn, D. I. Moon, T. J. Park, S. Y. Lee and Y. K. Choi, "An underlap field-effect transistor for electrical detection of influenza", Applied Physics Letters, 96, 033703, 2010.

[9] H. K. Hunt and A. M. Armani, "Label-free biological and chemical sensors", Nanoscale, 2, 1544-1559, 2010

[10] J. Homola, S. S. Yee, G. Gauglitz, "Surface plasmon resonance sensors: review", Sensors and Actuators B, 54, 3–15, 1999.

[11] H. R. Nejad, O. Z. Chowdhury, M. D. Buat and M. Hoorfar, " Characterization of the geometry of negative dielectrophoresis traps for particle immobilization in digital microfluidic platforms", Lab Chip, DOI: 10.1039/C3LC41292J.

[12] J. Lienemann, A. Greiner and J. G. Korvink, " Modeling, Simulation, and Optimization of Electrowetting", IEEE transactions on computer-aided design of integrated circuits and systems, 25, 234-247, 2006.